International Journal of Innovative
Computing, Information and Control
Volume 7, Number 12, December 2011

 ISSN 1349-4198
pp. 6691–6710

COLOR IMAGE ENHANCEMENT WITH EXACT HSI COLOR MODEL

Chun-Liang Chien and Din-Chang Tseng*

Institute of Computer Science and Information Engineering
National Central University
No. 300, Jungda Rd., Chungli 32001, Taiwan
93542014@cc.ncu.edu.tw; *Corresponding author: tsengdc@ip.csie.ncu.edu.tw

Received July 2010; revised January 2011

Abstract. *While enhancing the intensity or saturation component for high-quality color image enhancement, keeping the hue component unchanged is important; thus, perceptual color models such as HSI, HSL and HSV were used. Hue-Saturation-Intensity (HSI) is a public color model, and many color applications are commonly based on this model; however, the transformation from HSI model to RGB model usually generates the out-of-gamut problem after modifying intensity and saturation in the HSI model. Moreover, the saturation component is always increased or decreased following the change of intensity component no matter what the attainable saturation range is. In this paper, we propose accurate formulas for the color transformation between RGB and the proposed HSI color model, called the exact HSI (eHSI) color model, to resolve the out-of-gamut problem directly as well as automatically adapt the saturation range; that is, the saturation component can be enhanced or reduced according to the attainable maximum saturation range. In experiments, we demonstrate how to sacrifice a little contrast to improve the image saturation based on the proposed eHSI color model.*
Keywords: Color image enhancement, Out-of-gamut, Perceptual color model, Exact *HSI* color model

1. **Introduction.** Many color models have been proposed for various applications. Each color model has its own advantages and disadvantages. The popular color model *CIELAB* is perceptually uniform scaled but encounters the out-of-gamut problem. The hue-saturation-intensity (*HSI*) color model has human-intuitional advantages in image processing such as color image enhancement, segmentation, fusion, color-based object detection, recognition, traffic signal detection and skin detection, but also partially encounters the out-of-gamut problem.

The *HSI* model describes more exact color than *RGB* model describes for human interpretation [1]. Though the *HSI* model is non-uniform in perception, it is still one of the most popular color models for color image processing. More than 4,670 papers in recent four years (2006-2009) were extracted when we used "*HSI* color" as the keyword to search papers in "Google Scholar" web site. In practical applications, the non-uniformity in perception can be solved by some techniques. For example, in color image segmentation, the deformed boundaries can be used to enclose the target cluster so that the perception uniformity is not so critical. The out-of-gamut problem is really the knotty problem. This study just focuses on solving the out-of-gamut problem for color image enhancement and clarifying the drawback of the traditional *HSI* color model. The whole process is unconcerned with the perception uniformity.

Histogram equalization is a well-known image contrast enhancement method and has been used for various image enhancements [2-5]; however, it often produces images with

unnatural appearances and visually disturbing artifacts. One reason for the unwanted effect is that histogram equalization attempts to force the output image to have a uniform gray-level distribution regardless of what the original gray-level distribution is. A better solution should consider the original gray-level distribution to ensure that the output image not only has enhanced visibility and contrast but also is faithful to the original appearance. On the other hand, the hue components of the pixels should not be changed for color image enhancement. If we change the hue, the appearance of the original color is changed significantly, and then, the image color is distorted. For general hue-preserving color image enhancement, the original *RGB* image is usually transformed to another color space such as *HSI*, *LHS* or *HSV*; then, the intensity or saturation component is enhanced, but the hue component remains unaltered.

Though the transformation between *HSI* and *RGB* models is nonlinear, the transformation theoretically makes the intensity and saturation of manipulated pixels never out of gamut if the manipulation is limited in the range of $[0, 1]$. Furthermore, if a pixel's intensity is changed, its saturation component is automatically tuned according to the attainable maximum saturation range. Unfortunately, the *HSI* color system is deduced from the three low-intensity planes of the *RGB* cube so that the previous mentioned advantages are successfully achieved in low intensity portion but failed in high intensity portion [1]. Duan and Qiu [6] mentioned that, in the *HSI* color space, the attainable maximum saturation is actually a function of the intensity in the same hue plane as shown in Figure 1. We practiced color patch analysis and found that the complete *HSI* color model was distorted on the upper portion as shown in Figure 2(c).

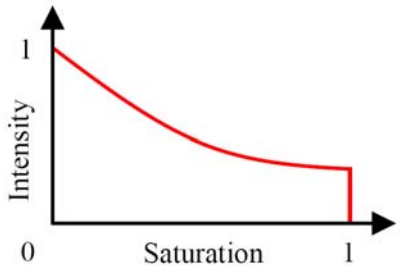

FIGURE 1. The attainable maximum saturation at different intensity values for a fixed hue region from 0° to 6°

This distortion makes several undesirable phenomena; for example, a pixel's saturation component is automatically increased after conversion from the *HSI* space to the *RGB* space with increased intensity. Hence, the pixel is possibly out of gamut. On the other hand, the saturation is always reduced if the intensity is reduced in the *HSI* color space, whether the attainable maximum saturation ranges are wide or narrow. Consequently, the intensity of an image is correct, but the saturation is decreased; then an extra saturation enhancement procedure is necessary. In the spectra of light, each color is at the maximum purity (or strength or richness) that eyes can appreciate, and the spectrum of colors is described as fully saturated. If a saturated color is diluted by mixing with other colors or white, the color's richness or saturation is decreased [7]. Hence, correct saturation enhancement will produce a more pleasant image. Several enhancement methods have been proposed; however, the enhancement of saturation is not so easy. For example, (*i*) the attainable maximum saturation range in the middle intensity region is wider than those in the high- and low-intensity regions so that enhancing saturation must be coordinated with the change of intensity; (*ii*) the histogram equalization may generate uneven enhanced results for large smooth segments in images; (*iii*) to avoid an oversaturated image, the

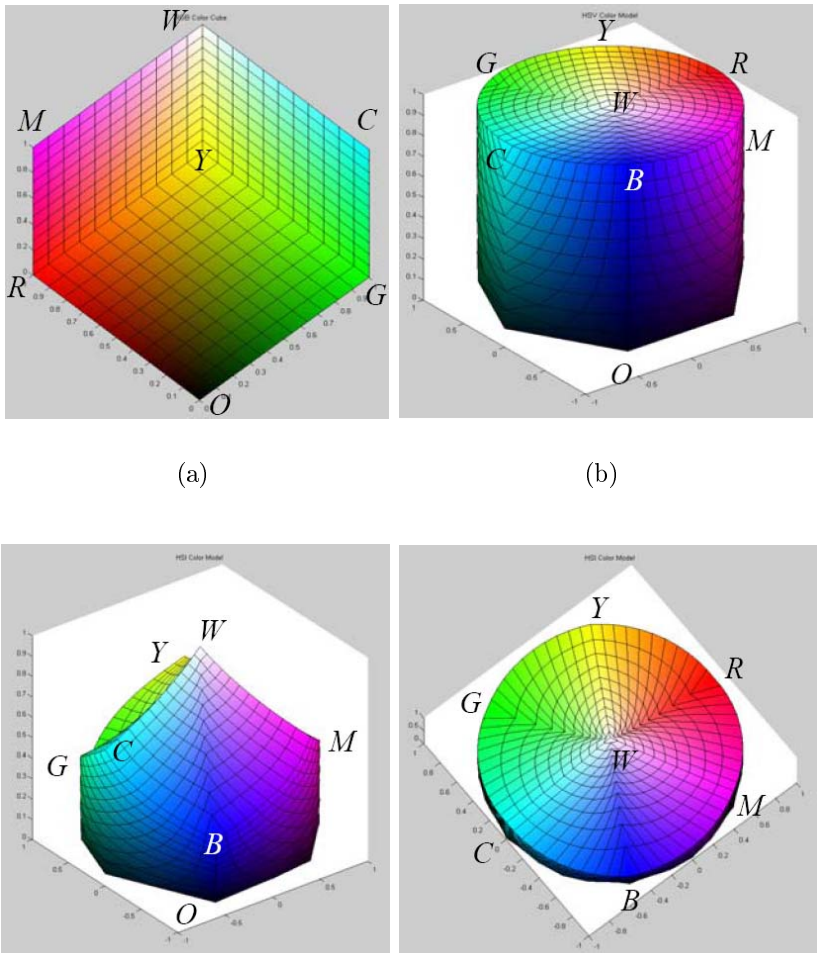

(a) (b)

(c) (d)

FIGURE 2. The color patch analysis: (a) the color patches of the *RGB* cube; (b) the color patches of the *HSV* color model; (c) the color patches of the *HSI* color model; (d) the top-viewed *HSI* color model

pixels in the achromatic segments must not be enhanced, but the achromatic segments are difficult to determine in the image.

Strickland et al. [8] proposed an enhancement scheme based on the fact that objects can exhibit variation in color saturation with little or no corresponding intensity variation. Thomas et al. [9] proposed an improvement over Strickland's method by considering the correlation between the intensity and saturation components of the image locally. Toet [10] also extended Strickland's method to incorporate all spherical frequency components by representing the original intensity and saturation components of a color image at multiple spatial scales. Pitas and Kiniklis [11] proposed a method to jointly equalize the intensity and saturation components. Trahanias and Venetsanopoulos [12] proposed a method of direct 3D histogram equalization that results in a uniform histogram of the *RGB* values. Mlsna and Rodriguez [13] proposed a multivariate enhancement technique, called "histogram explosion", in which the equalization procedure is performed on a series of rays emanating from a common point in a 3D histogram. This principle was later extended to the *CIE LUV* space [14]. The authors also proposed a recursive algorithm for 3D

histogram enhancement of color images [15]. Bockstein [16] proposed a color equalization method for both saturation and intensity.

Weeks et al. [17] proposed a hue-preserving color image enhancement technique that modifies the saturation and intensity components in a color difference (C-Y) space. At first, an image is transformed into the C-Y color space (e.g., $YCbCr$) and then segmented into N hue regions and K luminance regions. To avoid the out-of-gamut problem, the values for the maximum realizable saturation $S\max(n,k)$, $n = 1, 2, 3, \ldots, N$ and $k = 1, 2, 3, \ldots, K$, are computed by searching all possible RGB combinations and selecting the corresponding maximum saturation value for the hue-intensity combination. This computation is performed once for the desired number of regions, and then the results are stored in a table where the values can be used repeatedly by the equalization algorithm. The authors proposed two methods to equalize the intensity and chromatic components. The first method equalizes the intensity and then equalizes the saturation component based on the enhanced intensity. The second method equalizes the saturation component and then equalizes the intensity component by referring to the enhanced saturation. The different order affects the intensity value if the saturation is limited in the saturation equalization process. The first method may generate images with high contrast and brightness but low saturation. The result comes from increasing the overall range of luminance but limiting the maximum realizable saturation. The second method tends to produce images with high saturation but low brightness and contrast because the high-saturated color limits the allowed intensities in the RGB space to a small range. Duan and Qiu [6] mentioned that the more the regions are divided, the fewer cross-session artifacts there are, but more computational time is needed. Each method has its own advantages and disadvantages, but there is no specific criterion to decide which component should be enhanced first. In addition, there is no specific criterion for deciding the parameters N and K; moreover, calculating the lookup table is complicated.

Yang and Rodriguez [18] proposed two hue-preserving techniques, scaling and shifting, for processing intensity and saturation components. To implement the techniques, all pixels are processed in the RGB space; this means that transformation of the color coordinates is not necessary. Later, the authors also developed clipping techniques [19] in the LHS and YIQ spaces for enhancement by dealing in particular with the values that fall outside the range of the RGB space, where clipping is performed after the enhancement. Rodriguez and Yang [20] also proposed a high-resolution histogram equalization of color images. The effect of quantization error in the luminance quantization has been studied in detail.

Naik and Murthy [21] indicated that, though the mentioned algorithms are effective for enhancement, most do not effectively take care of the gamut problem in which the pixel values go beyond the boundaries after processing. Due to the nonlinear nature of uniform color spaces, conversion from these spaces with modified intensity and saturation values to the RGB space generates the gamut problem. In general, the problem is tackled by either clipping the out-of-boundary values to the boundaries or normalizing the entire intensity and saturation ranges [16]. Clipping the values to the boundaries creates an undesired shift in the hue. Strickland et al. [8] also discussed the clipping problem. Normalization reduces the intensity achieved in the enhancement process, which defeats the original objective [22].

Weeks et al. [17] mentioned that the color enhancement procedure usually suffers from not only the out-of-gamut problem but also the contradiction between intensity and saturation. To resolve both problems, we propose an exact HSI ($eHSI$) color model that not only prevents pixels from going out of gamut but also adaptively adjusts the saturation according to the ratio of the target and the source attainable maximum saturation range

rather than following the intensity change. In the proposed approach, a color image is first transformed from *RGB* to the proposed *eHSI* color space. Then, we use histogram stretching or histogram equalization to expand the intensity histogram and enhance the contrast of the color images. On the other hand, to enhance the saturation, we may deform the shape of the intensity histogram by moving the intensity mean to the central point (e.g., 128 for 256 gray scales) and then stretching the intensity range on one side of the mean and compressing that on the other side of mean. This operation makes more pixels fall into the region with "larger saturation expansion range" in the color space. Some histograms are dispersed such as a bi-modal histogram with two peaks locating near the two ends, so that the previous operation is useless. Thus, if the saturation enhancement result is not very conspicuous, we can add an *S-type* transformation [21] to concentrate the intensity in the central region which has a larger saturation range. Then, the image is conversed back to the *RGB* space to complete the enhancement.

The remaining sections of this paper are organized as follows. Section 2 describes the color patch analysis, which is a visual tool and will be used to recognize the shape of different color models; we use the tool to verify the correctness of the proposed *eHSI* color model. The proposed *eHSI* to *RGB* transformation is derived and presented in Section 3; the *RGB* to *eHSI* transformation is derived and presented in Section 4. The difference between the *eHSI* and the traditional *HSI* color models is analyzed and discussed in Section 5. We found that the out-of-gamut problem in the traditional *HSI* color model could be completely resolved in the proposed *eHSI* color model, but the saturation of high- or low-intensity pixels is still reduced when they are converted back to the *RGB* space. Thus, an *S-type* transformation is used to enhance the saturation by sacrificing a little contrast of intensity as presented in Section 6. Several practical enhancement experiments are discussed and reported in Section 7. Finally, conclusions are given in Section 8.

2. **Color Patch Analysis.** Converting color from *RGB* to the traditional *HSI* is defined as [1]:

$$\begin{cases} I = \dfrac{R+G+B}{3} \\ H = \begin{cases} \theta, & \text{if } B \le G \\ 360^\circ - \theta, & \text{if } B > G \end{cases} \\ \qquad \text{with } \theta = \cos^{-1}\left\{ \dfrac{\frac{1}{2}\left[(R-G)+(R-B)\right]}{\left[(R-G)^2+(R-B)(G-B)\right]^{1/2}} \right\} \\ S = 1 - \dfrac{3}{R+G+B}\min(R,G,B) \end{cases}, \tag{1}$$

where I and S are in the range of $[0, 1]$ and H is in the range of $[0, 360]$.

To convert color from the *HSI* to *RGB*, three cases of the H range must be considered. *RG* section: $0^\circ \le H < 120^\circ$

$$\begin{cases} B = I(1-S) \\ R = I\left[1 + \dfrac{S\cos H}{\cos(60^\circ - H)}\right] \\ G = 3I - (R+B) \end{cases}. \tag{2}$$

GB section: $120^\circ \leq H < 240^\circ$

$$H = H - 120^\circ$$
$$\begin{cases} R = I\,(1 - S) \\ G = I\left[1 + \dfrac{S\cos H}{\cos\,(60^\circ - H)}\right] \\ B = 3I - (R + G) \end{cases} . \tag{3}$$

BR section: $240^\circ \leq H < 360^\circ$

$$H = H - 240^\circ$$
$$\begin{cases} G = I\,(1 - S) \\ B = I\left[1 + \dfrac{S\cos H}{\cos\,(60^\circ - H)}\right] \\ R = 3I - (G + B) \end{cases} . \tag{4}$$

To understand the relationship between the *HSI* and *RGB* models, we divided each surface plane of the *RGB* cube into $11 \times 11 = 121$ patches. The vertices of every color patch are defined by their *RGB* coordinates. The color in every patch is calculated by interpolation of its four vertices with the reciprocal of the distance as the interpolation weight as illustrated in Figure 2(a). We then transfer the vertex coordinates of all patches into other color spaces such as *HSI* or *HSV* color space and keep the vertices and face colors unchanged. The transferred *HSV* color model is illustrated in Figure 2(b), and the transferred *HSI* color model is illustrated in Figures 2(c) and 2(d). The lower part of the *HSI* model is cylindrical (you may look the hexagonal shape at the bottom due to the discrete patches), but the upper part is deformed because the *HSI* color transformation is deduced from the three low-intensity planes of the *RGB* cube (i.e., the *ORYG*, *OGCB* and *OBMR* planes) as illustrated in Figure 2(a); thus, the three high-intensity planes (i.e., the *WYRM*, *WMBC* and *WCGY* planes) are distorted.

This distorted model will generate several unusual phenomena after the intensity is enhanced. First, the color of a pixel may go out of gamut. If the intensity or saturation of some pixels is increased so that they are out of the top surface of the *HSI* model, the out-of-gamut problem will be generated when they are transformed back to the *RGB* space. Second, if a pixel's intensity is increased by an enhancement procedure, the pixel's saturation will be linearly expanded; on the other hand, if a pixel's intensity is decreased, the pixel's saturation will be linearly shrunk whether the target saturation range is wider or narrower. The details will be described in Section 5.1.

To resolve the out-of-gamut and shrunken saturation problems, we improved the *HSI* color transformation formulas. The idea is that if the intensity is higher than certain boundaries, then the *HSI* formulas will be derived from the three high-intensity planes in the *RGB* cube (i.e., the *WYRM*, *WMBC* and *WCGY* planes) as illustrated in Figure 2(a).

3. ***RGB* to *eHSI* Transformation.** We can derive the saturation for the *eHSI* model based on the geometric structure of the *RGB* cube as shown in Figure 3(b). In the figure, an arbitrary color point p has coordinates (R, G, B) and is located on the triangle $C'M'Y'$ that is perpendicular to the black-white gray axis and intersects the axis at u point. The saturation of a color is defined as the degree to which the color is diluted by white; thus, the saturation S of color point p is given by the ratio $|\overline{up}| \,/\, |\overline{up'}|$, where p' is the intersection of the extension of $\overline{up}$ line and one border of the triangle $C'M'Y'$. Let t be the orthogonal projection of u on the *WCM* plane, and let q be the orthogonal projection

of p on the $\overline{ut}$ line. According to the two similar triangles Δupq and $\Delta up't$, we have

$$S = \frac{|\overline{up}|}{|\overline{up'}|} = \frac{|\overline{uq}|}{|\overline{ut}|} = \frac{|\overline{ut}| - |\overline{qt}|}{|\overline{ut}|}. \tag{5}$$

From Figure 3(b), we can find that q and p have the same B value; thus, $|\overline{qt}| = 1 - B$. Furthermore, we can find that the length $|\overline{Wu}|$ is

$$|\overline{Wu}| = \frac{\overline{Wp} \cdot (1,1,1)}{|(1,1,1)|} = \frac{(1-R)+(1-G)+(1-B)}{\sqrt{3}}. \tag{6}$$

If the coordinate of u is (ω, ω, ω), then $|\overline{ut}|$ is $1 - \omega$. Since

$$|\overline{Wu}| = \sqrt{3\,(1-\omega)^2} = \frac{(1-R)+(1-G)+(1-B)}{\sqrt{3}} = \sqrt{3}(1-I), \tag{7}$$

then

$$1 - \omega = \frac{(1-R)+(1-G)+(1-B)}{3} = 1 - I. \tag{8}$$

That is,

$$|\overline{ut}| = \frac{(1-R)+(1-G)+(1-B)}{3} = 1 - \frac{(R+G+B)}{3} = 1 - I \tag{9}$$

in the presented (CM) section; thus,

$$S = 1 - \frac{3\,(1-B)}{3-(R+G+B)}. \tag{10}$$

From Figures 2(a) and 3(b), we can find $B = \max(R, G, B)$ in the CM section. Hence, the saturation can be formularized as

$$S = 1 - \frac{3\,(1-\max\,(R,G,B))}{3-(R+G+B)}. \tag{11}$$

The same results can be acquired for the two other sections, the MY and YC sections, with a similar derivation.

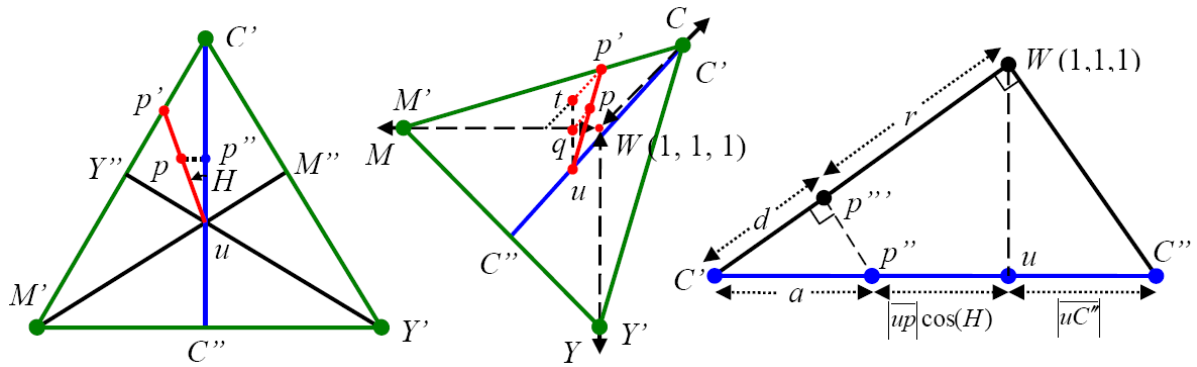

FIGURE 3. Details of the *eHSI* triangle for acquiring an accurate saturation component: (a) the top view of the $C'M'Y'$ triangle; (b) oblique top view for deriving *RGB* to *eHSI* conversion formulas; (c) side view for deriving *eHSI* to *RGB* conversion formulas

In applications, we must have a criterion to judge using the traditional saturation formula or the proposed saturation formula. That is, if the attainable maximum saturation of a pixel is located in the three high-intensity planes of the *RGB* cube, then the pixel's

saturation should be calculated by the proposed saturation calculation; otherwise, the pixel's saturation is calculated by the traditional saturation calculation. The boundary between the traditional saturation and the new saturation regions is shown in Figure 4. Based on the intensity and hue values, if a pixel is above the boundary, the new formula is used; otherwise, the traditional formula is used. In practice, we divide the hue range into three sections ($[0, 120]$, $[120, 240]$ and $[240, 360]$) and then use the central point of each section as the reference point. If a pixel's hue angle is equal to the central point (i.e., 60°, 180° or 300°) and the pixel's intensity is greater than 1/3, then the new saturation formula is used. On the other hand, if a pixel's hue angle is equal to the boundary point of each section (i.e., 0°, 120° or 240°) and the pixel's intensity is greater than 2/3, then the new saturation formula is used. Hence, the calculation of saturation accompanying the decision criterion is summarized as

$$\begin{cases} H = H \bmod 120^\circ \\ \text{if } I > \dfrac{2}{3} - \dfrac{abs\,(H - 60^\circ)}{180^\circ}, & \text{then } S = 1 - \dfrac{3\,(1 - \max\,(R, G, B))}{3 - (R + G + B)} \\ & \text{else } S = 1 - \dfrac{3}{R + G + B} \min\,(R, G, B)\,. \end{cases} \tag{12}$$

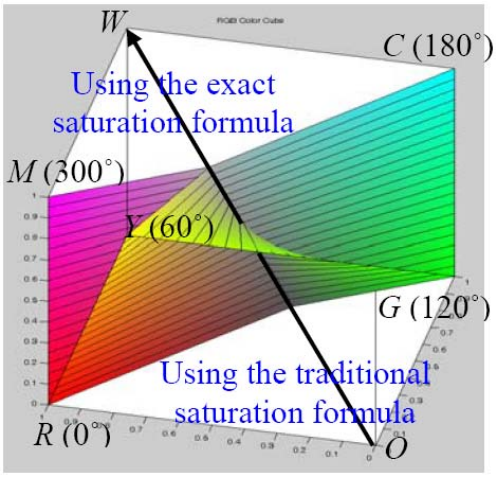

FIGURE 4. The boundary for determining to use the traditional saturation formula or the exact saturation formula. If a pixel is located under the boundary, the pixel's saturation is calculated by the traditional *HSI* formulas; otherwise, the pixel's saturation is calculated by the proposed *eHSI* formulas.

The computational burden of the transformation from *RGB* to *eHSI* is not much higher than to the traditional *HSI* since the extra load is just the calculation "$H = H \bmod 120°$" and the decision in Equation (12).

We have transformed the color patches on the *RGB* cube to the *eHSI* model as illustrated in Figure 5. The upper portion of the *eHSI* model is a perfect cylinder; that is, the *eHSI* model is undistorted and is correct.

4. ***eHSI* to *RGB* Transformation.** We need conversion formulas from *eHSI* to *RGB* after the processing is completed in the *eHSI* color space. The traditional transformation is separated into three cases: the *RG*, *GB* and *BR* sections to convert *HSI* to *RGB*. For the *eHSI* to *RGB* transformation, we must consider six cases: the *RG*, *GB*, *BR*, *CM*, *MY* and *YC* sections. The former three cases are the same as the traditional transformation,

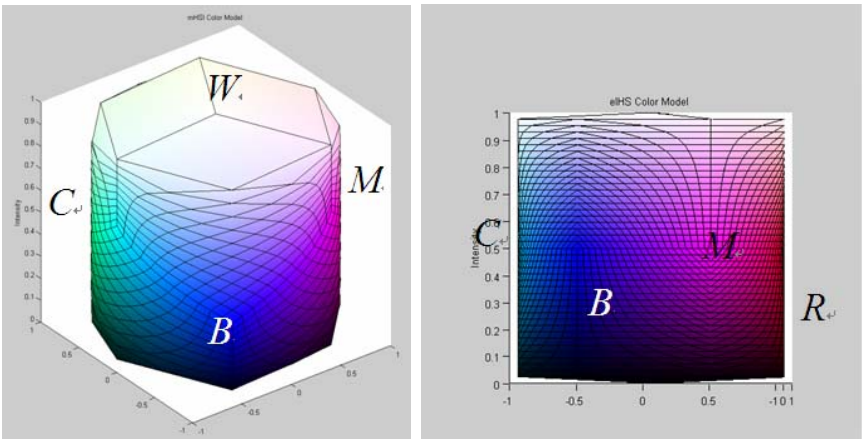

(a) (b)

FIGURE 5. The color patches of the *eHSI* color model: (a) the oblique top view; (b) the side view

but the intensity component must be restricted. That is,

the RG section: $0^\circ < H \leq 120^\circ$ & $I \leq \dfrac{2}{3} - \dfrac{abs\,(H - 60^\circ)}{180^\circ}$

$$\begin{cases} B = I\,(1 - S) \\ R = I\left[1 + \dfrac{S\cos H}{\cos\,(60^\circ - H)}\right] \\ G = 3I - (R + B) \end{cases}. \tag{13}$$

The GB section: $120^\circ < H \leq 240^\circ$ & $I \leq \dfrac{2}{3} - \dfrac{abs\,(H - 180^\circ)}{180^\circ}$

$$H = H - 120^\circ$$

$$\begin{cases} R = I\,(1 - S) \\ G = I\left[1 + \dfrac{S\cos H}{\cos\,(60^\circ - H)}\right] \\ B = 3I - (R + G) \end{cases}. \tag{14}$$

The BR section: $240^\circ < H \leq 360^\circ$ & $I \leq \dfrac{2}{3} - \dfrac{abs\,(H - 300^\circ)}{180^\circ}$

$$H = H - 240^\circ$$

$$\begin{cases} G = I\,(1 - S) \\ B = I\left[1 + \dfrac{S\cos H}{\cos\,(60^\circ - H)}\right] \\ R = 3I - (G + B) \end{cases}. \tag{15}$$

For the CM, MY and YC sections, the conversion formulas should be modified based on the 3D geometric structure of the CM, MY and YC sections. For the CM section ($180^\circ < H \leq 300^\circ$), the S component can be derived from Equation (10); that is,

$$S = 1 - \frac{1 - B}{1 - I}, \tag{16}$$

then

$$B = I\,(1 - S) + S. \tag{17}$$

From Figures 3(b) and 3(c), we can find that the value of r is the orthogonal projection of $\overline{Wp}$ on the C axis. Consider the triangle $\Delta C'WC''$ shown in Figure 3(c), where W is the highest point $(1,1,1)$ of the RGB coordinate system. From the two similar triangles $\Delta C'WC''$ and $\Delta C'P'''P''$, we have

$$\frac{\left|\overline{C'C''}\right|}{\left|\overline{C'W}\right|} = \frac{a}{d}, \tag{18}$$

where p'' is the orthogonal projection of p on the $\overline{C'C''}$ line, and p'' is the orthogonal projection of p'' on the $\overline{C'W}$ line. We derived the length $\left|\overline{Wu}\right|$ in Equation (7). Accordingly, if the coordinates of C' are $(\delta,1,1)$, then the length of $\left|\overline{C'W}\right|$ is equal to $1-\delta$. Since

$$\frac{((1,1,1)-(\delta,1,1))\cdot(1,1,1)}{|(1,1,1)|} = \frac{1-\delta}{\sqrt{3}} = \left|\overline{Wu}\right|; \tag{19}$$

hence,

$$\overline{|C'W|} = \sqrt{3}\left|\overline{Wu}\right| = (1-I). \tag{20}$$

From Figures 3(a) and 3(c) and Equation (20), we have

$$d = \left|\overline{C'W}\right| - r, \tag{21}$$

$$a = \left|\overline{C'C''}\right| - \left(|\overline{up}|\cos H + \left|\overline{uC''}\right|\right), \tag{22}$$

and

$$\left|\overline{C'C''}\right| = 3\left|\overline{uC''}\right|. \tag{23}$$

Substituting Equations (18), (20), (22) and (23) into Equation (21) and simplifying yields

$$\begin{aligned} r &= \left|\overline{C'W}\right| - d = \left|\overline{C'W}\right| - \frac{a\left|\overline{C'W}\right|}{\left|\overline{C'C''}\right|} = \left|\overline{C'W}\right|\left(\frac{|\overline{up}|\cos H + \left|\overline{uC''}\right|}{\left|\overline{C'C''}\right|}\right) \\ &= 3(1-I)\left(\frac{1}{3} + \frac{|\overline{up}|\cos H}{\left|\overline{C'C''}\right|}\right) = (1-I)\left(1 + \frac{3\,|\overline{up}|\cos H}{\left|\overline{C'C''}\right|}\right). \end{aligned} \tag{24}$$

The only unknown in this equation is $|\overline{up}|$. In Figure 3(a), we know that $|\overline{up}| = S\left|\overline{up'}\right|$. At u, the angle included by the line segments $\overline{uC'}$ and $\overline{uY''}$ is 60°; thus, $\left|\overline{up'}\right| = \left|\overline{uY''}\right| / \cos(60^\circ - H)$. We know that $\left|\overline{uY''}\right| = \left|\overline{uC''}\right|$; hence, $\left|\overline{up'}\right| = \left|\overline{uC''}\right| / \cos(60^\circ - H)$. Substituting these results and Equation (23) into Equation (24) yields

$$\begin{aligned} r &= (1-I)\left(1 + \frac{3S\left|\overline{up'}\right|\cos H}{\left|\overline{C'C''}\right|}\right) = (1-I)\left(1 + \frac{3S\left|\overline{uC''}\right|\cos H}{\left|\overline{C'C''}\right|\cos(60^\circ - H)}\right) \\ &= (1-I)\left(1 + \frac{S\cos H}{\cos(60^\circ - H)}\right). \end{aligned} \tag{25}$$

As illustrated in Figures 2(a) and 3(c), the coordinates of W are $(1,1,1)$; thus, R can be obtained by

$$R = 1 - r = 1 - (1-I)\left(1 + \frac{S\cos H}{\cos(60^\circ - H)}\right). \tag{26}$$

Since $I = (R+G+B)/3$, we then have

$$G = 3I - (R+B). \tag{27}$$

Similar results can be acquired for the MY and YC sections in the same derivation manner. The final conversion formulas for the YC, CM and MY sections are summarized

as follows.

The YC section: $60^\circ < H \leq 180^\circ$ & $I > \dfrac{1}{3} + \dfrac{abs\,(H - 120^\circ)}{180^\circ}$

$$H = H - 240^\circ$$
$$\begin{cases} G = I\,(1 - S) + S \\ B = 1 - (1 - I)\left[1 + \dfrac{S\cos H}{\cos\,(60^\circ - H)}\right] \\ R = 3I - (G + B) \end{cases} . \tag{28}$$

The CM section: $180^\circ < H \leq 300^\circ$ & $I > \dfrac{1}{3} + \dfrac{abs\,(H - 240^\circ)}{180^\circ}$

$$\begin{cases} B = I\,(1 - S) + S \\ R = 1 - (1 - I)\left[1 + \dfrac{S\cos H}{\cos\,(60^\circ - H)}\right] \\ G = 3I - (R + B) \end{cases} . \tag{29}$$

The MY section: $\left(300^\circ < H \leq 360^\circ \;\&\; I > \dfrac{1}{3} + \dfrac{360^\circ - H}{180^\circ}\right)$ or $\left(0^\circ < H \leq 60^\circ \;\&\; I > \dfrac{1}{3} + \dfrac{H}{180^\circ}\right)$

$$H = H - 120^\circ$$
$$\begin{cases} R = I\,(1 - S) + S \\ G = 1 - (1 - I)\left[1 + \dfrac{S\cos H}{\cos\,(60^\circ - H)}\right] \\ B = 3I - (R + G) \end{cases} . \tag{30}$$

The MY section is across 0° boundary, so hue angles less than 0° and greater than 0° should be considered with different intensity ranges.

The computational burden of the transformation from *eHSI* to *RGB* is also not much higher than from the traditional *HSI* since the extra load is only the decision for Equations (13)-(15) and Equations (28)-(30).

We also used the previous patch analysis to verify the correctness of the *eHSI* to *RGB* transformation. The reversed *RGB* cube is completely the same as the original *RGB* cube; thus, we confirmed that the proposed *eHSI* to *RGB* transformation is correct. The proposed new *HSI* color model creates an exact color transformation between *RGB* and *HSI*; thus we call it the exact *HSI* (*eHSI*) color model.

5. The Influence of Intensity on Saturation in *HSI* and *eHSI* Color Spaces.

We use a geometric graph to explore the co-variation of intensity and saturation in the *HSI* and the *eHSI* color spaces. Moreover, we use a color palette to verify the correctness of the relationship between intensity and saturation.

5.1. The influence of intensity on saturation.

We have stated that the traditional *HSI* is derived from the low-intensity planes of the *RGB* cube. Since the three planes are expanded outward as the intensity is increased, we speculate that the saturation is always enhanced as the intensity is increased. As illustrated in Figure 6(a), if the intensity of pixel a is increased from L_1 to L_2 in the *HSI* color space, this means that pixel a is transferred to b. In this case, b is out of gamut, but actually, the pixel's intensity is bounded by the *RGB* cube and cannot reach the L_2 level. On the other hand, if the intensity of pixel c is decreased from L_2 to L_1, the pixel's location is transferred to d, and the pixel's saturation is always decreased.

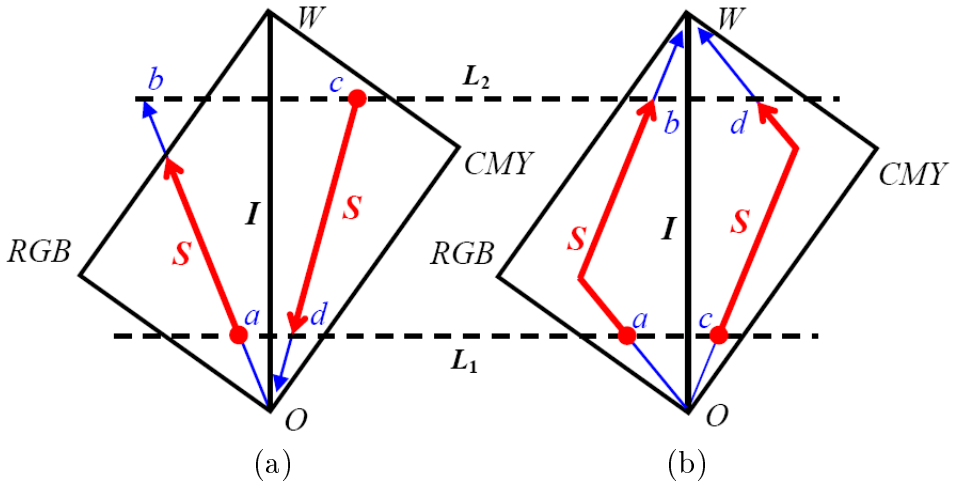

FIGURE 6. The saturation variation coincides with the intensity change: (a) saturation change in the *HSI* color space; (b) saturation change in the *eHSI* color space

In the proposed *eHSI* color model, the maximum saturation is coincident with the attainable maximum saturation range in the *RGB* space; the out-of-gamut problem is solved and the saturation is adjusted according to the attainable maximum saturation range. As illustrated in Figure 6(b), if the intensities of pixels a and c are increased from L_1 to L_2, their locations are transferred to b and d, respectively; but the pixels' saturations are adaptively changed according to the border structure of the color space. The saturation expansion range for d is wider than for c, so the pixel's saturation is enhanced; on the other hand, the saturation expansion range for b is narrower than that for a, so the pixel's saturation is reduced. In the *eHSI* space, there is no out-of-gamut problem, and the change in saturation depends completely on the relative saturation ranges of the target and the original intensity levels. In image enhancement, if the saturation range of the target intensity level is greater than that of the original intensity level, the saturation is enhanced; otherwise, the saturation is reduced. This is beneficial for saturation enhancement; that is, if we sacrifice a little contrast and push the pixel's intensity toward the central region on the intensity axis, the saturation is automatically enhanced.

5.2. **Quantitative evaluation.** To quantitatively evaluate the influence of intensity on saturation while the intensity is being adjusted, we create a color palette with six rectangle color blocks to verify the proposed transformation as illustrated in Figure 7(a). The six colors are the pure R, Y, G, C, B and M; their hues are just 0°, 60°, 120°, 180°, 240° and 300°. Every color block is divided into left and right squares. All six left squares have 1/3 the intensity and the maximum saturation, and all six right squares have 1/6 the intensity and 1/2 the maximum attainable saturation. In the figure, there are two real numbers in each square; the upper number is the intensity, and the lower number is the saturation. The intensity is in the range of $[0, 1]$ and the saturation value is calculated from the geometric distance on the *RGB* cube.

The saturation calculation of the high-intensity portion is different for the *HSI* and the *eHSI* color spaces. To compare the results, we must unify the saturation values by using the geometric distance on the *RGB* cube as the unit. As illustrated in Figure 8, the length of the intensity axis ($\overline{OW}$ axis) is $\sqrt{3}$. The saturation value is directly calculated from the perpendicular distance to the intensity axis. The orthogonal projection of p on the

$\overline{OW}$ axis is

$$\frac{(R,G,B)\cdot(1,1,1)}{\sqrt{3}} = \frac{R+G+B}{\sqrt{3}}, \tag{31}$$

so that the perpendicular distance S is

$$S = \sqrt{R^2+G^2+B^2-\frac{(R+G+B)^2}{3}} = \sqrt{\frac{(R-B)^2+(B-G)^2+(G-R)^2}{3}}. \tag{32}$$

For example, the saturation of $(1,0,0)$ in the traditional representation is 1, but here the saturation will become

$$\sqrt{\frac{(1-0)^2+(0-0)^2+(0-1)^2}{3}} = \sqrt{\frac{2}{3}} \cong 0.8165.$$

Next, we add 1/3 to the intensity of every rectangle block of the color palette; that is, the intensity of the left squares becomes 2/3, and that of the right squares becomes 1/2. According to the previous analysis, we predict that, in the *HSI* color space, the pure R, G and B pixels will become out of gamut after their intensity exceeds 1/3. As shown in Figure 7(b), the intensity and saturation of the left squares of the R, G and B blocks are not changed, but those of the right squares are enhanced. This is an unusual phenomenon that the intensity of the right squares exceeds that of the left squares after the intensity is increased because the left squares are out of gamut and bounded by the *RGB* cube. On the other hand, the intensity and saturation of the C, Y and M blocks are all enhanced. Contrary to the *HSI* color space, the intensity in the *eHSI* color space is normally changed as illustrated in Figure 7(c); the saturation of all the squares is increased or decreased according to the attainable saturation range as described in Figure 6(b).

Another analysis is illustrated in Figure 7(d). The left square of every rectangle block has 2/3 the intensity and the maximum saturation, and all six right squares have 1/2 the intensity and the maximum attainable saturation. Now, we subtract 1/6 from the intensity of every rectangle block. In the *HSI* color space, the intensity and saturation of all blocks are all reduced as illustrated in Figure 7(e). Contrarily, in the *eHSI* color space, the intensity of all blocks is reduced, but the saturations of the R, G and B blocks are enhanced as illustrated in Figure 7(f). The target saturation expansion range is wider than the source expansion range.

6. **Compromise between Intensity and Saturation.** Along the intensity axis, the central region of the *RGB* cube has the widest saturation expansion range, and if we centralize the intensity in this region, the image will become more saturated. As illustrated in Figure 9(a), we observed that the intensity between P and Q has a wider saturation expansion range. In the general definition, one edge length of the *RGB* cube is 1, and the length of $\overline{RW}$ is equal to the diagonal of one square surface of the *RGB* cube; that is, $\left|\overline{RW}\right| = \sqrt{1^2+1^2} = \sqrt{2}$, and the length $\left|\overline{OW}\right| = \sqrt{2+1^2} = \sqrt{3}$. From similar triangles ΔWRP and ΔORP, we have

$$\left|\overline{OW}\right|/1 = 1/\left|\overline{OP}\right|. \tag{33}$$

Since $\left|\overline{OW}\right| = \sqrt{3}$, $\left|\overline{OP}\right| = 1/\sqrt{3}$ and $\left|\overline{OW}\right|/\left|\overline{OP}\right| = 3$. Hence, we conclude that the central 1/3 of the intensity range (i.e., from $\left|\overline{OW}\right|/3$ to $2\left|\overline{OW}\right|/3$) has a wider saturation expansion range. Moreover, we observe that, in this central range, the attainable maximum saturation range is from b to a; at the R (or G, B) or C (or Y, M) point, the

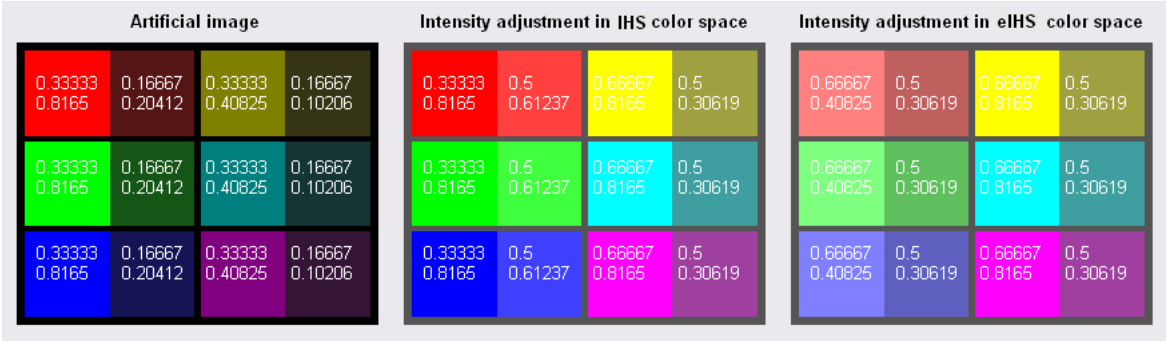

FIGURE 7. The influence of intensity on saturation. There are two real numbers in each square; the upper number is the intensity, and the lower number is the saturation: (a) a low-intensity artificial image; (b) the intensity is increased 1/3 in the *HSI* color space; (c) the intensity is increased 1/3 in the *eHSI* color space; (d) a high-intensity artificial image; (e) the intensity is decreased 1/6 in the *HSI* color space; (f) the intensity is decreased 1/6 in the *eHSI* color space.

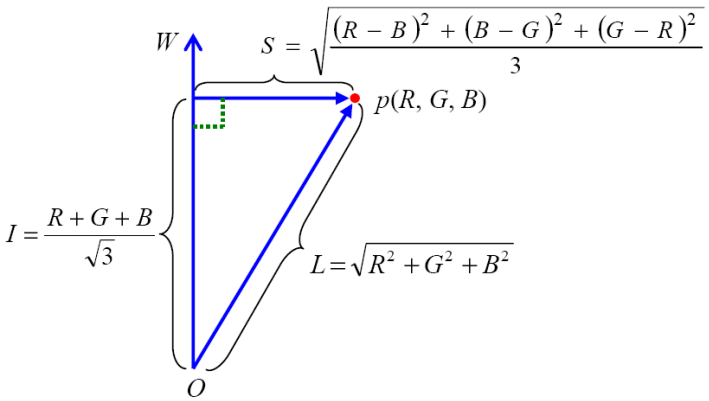

FIGURE 8. The calculation of intensity and saturation is based on the geometric distance of the *RGB* cube

attainable maximum saturation range is from c to a, where

$$\begin{cases} \dfrac{a}{1} = \dfrac{|\overline{WR}|}{|\overline{OW}|} = \dfrac{\sqrt{2}}{\sqrt{3}} & \Rightarrow \quad a = \dfrac{\sqrt{2}}{\sqrt{3}} = \dfrac{4\sqrt{6}}{12} \\ \dfrac{b}{|\overline{OW}|/2} = \dfrac{1}{|\overline{WR}|} \Rightarrow \dfrac{b}{\sqrt{3}/2} = \dfrac{1}{\sqrt{2}} & \Rightarrow \quad b = \dfrac{\sqrt{3}}{2\sqrt{2}} = \dfrac{3\sqrt{6}}{12} \\ \dfrac{c}{|\overline{OW}|/3} = \dfrac{1}{|\overline{WR}|} \Rightarrow \dfrac{c}{\sqrt{3}/3} = \dfrac{1}{\sqrt{2}} & \Rightarrow \quad c = \dfrac{\sqrt{3}}{3\sqrt{2}} = \dfrac{2\sqrt{6}}{12} \end{cases} . \tag{34}$$

According to the previous analysis, we know that there is a conflict between saturation and contrast; that is, some intensity enhancement processes such as intensity histogram equalization and stretching generally expand the intensity over the entire range as much as possible. These intensity adjustments will make some pixels unsaturated if they have high or low intensity. On the other hand, if we centralize the intensity to the central intensity region, the image will be more saturated, but the contrast may be reduced. In some conditions, perhaps we can sacrifice a little contrast to improve the saturation. As illustrated in Figure 9(a), the central range has a wider saturation expansion range. We can shift the mean of the intensity to the center point and/or use an *S-type* transformation to centralize the intensity in the central region. As illustrated in Figure 9(b), the *S-type* transformation can be set as

$$f(x) = \begin{cases} 0.5\left(\dfrac{x}{0.5}\right)^n, & 0 \le x \le 0.5 \\ 1 - 0.5\left(\dfrac{1-x}{0.5}\right)^n, & 0.5 < x \le 1 \end{cases}, \tag{35}$$

where n is a constant. If $n = 0.5$, Equation (35) can be simplified as

$$f(x) = \begin{cases} \sqrt{0.5x}, & 0 \le x \le 0.5 \\ 1 - \sqrt{0.5(1-x)}, & 0.5 < x \le 1 \end{cases}, \tag{36}$$

as shown in Figure 9(b).

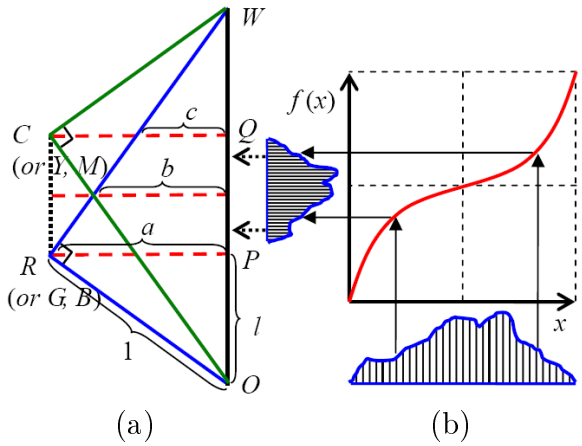

FIGURE 9. The saturation is enhanced by using an *S-type* transformation to centralize the intensities to the intensity center area where the attainable maximum saturation range is wider: (a) the side view of the *RGB* cube; (b) the *S-type* transformation

7. **Experiments.** Three color models: *HSI*, *CIELAB* and *eHSI* and two enhancement methods: histogram equalization and *S-type* transformation were compared for color image enhancement quality.

If an image is high bright, the intensity of most pixels is reduced after intensity histogram equalization. According to the previous analysis, the saturation will be also reduced in the *HSI* color space. As illustrated in Figure 10, the contrast of the Tiffany image is enhanced, but the saturation is deteriorated after intensity histogram equalization in the *HSI* color space, as shown in Figure 10(b). The similar result was obtained as shown in Figure 10(d), where L histogram of the *CIELAB* color model is equalized. Contrarily, the contrast and saturation are enhanced, as shown in Figure 10(f), where

intensity histogram of *eHSI* model was equalized. If the *S-type* transformation instead of the histogram equalization is applied on the intensity histogram of *HSI*, *CIELAB* and *eHSI* models, we also get the similar results as shown in Figures 10(c), 10(e) and 10(g), respectively. The saturation in *HSI* and *CIELAB* models is not adapted to the attainable maximum saturation range; as shown in Figures 10(c) and 10(e). However, with the *eHSI* model, the contrast is slightly reduced, but the color is more saturated, as shown in Figure 10(g).

We used a cosmetic image to conduct another experiment as shown in Figures 11 and 12. We artificially brightened and darkened the original cosmetic image to evaluate the enhancement effect, respectively. With the traditional *HSI* model, the brightened image becomes less saturated after intensity histogram equalization and the *S-type* transformation as illustrated in Figures 11(c) and 11(d), respectively. With the *CIELAB* model, the saturation is slight reduced after L histogram is equalized and processed by the *S-type* transformation as shown in Figures 11(e) and 11(f), respectively. With the *eHSI* model, the saturation of the brightened image is further enhanced after intensity histogram is equalized and processed by the *S-type* transformation as illustrated in Figures 11(g) and 11(h), respectively.

On the other hand, the darkened cosmetic image becomes oversaturated after the intensity histogram is equalized and centralized by the *S-type* transformation as illustrated in Figures 12(b) and 12(c), respectively. In the results, the out-of-gamut problem limits the increase in intensity so that intensity does not reach the desired value (e.g., the white color panel) and the contrast is limited (e.g., the texture of red color panel). With the *CIELAB* model, the contrast is enhanced but saturation is unchanged after L histogram is equalized and centralized by the *S-type* transformation as shown in Figures 12(d) and 12(e), respectively. Contrarily, there are no out-of-gamut and oversaturation problems with the same enhancements on the *eHSI* model as shown in Figures 12(f) and 12(g), respectively; moreover, intensity and contrast can reach the desired levels.

Here, we conclude that the intensity enhancement of high-saturated images in the *eHSI* space is better than that in the traditional *HSI* space. Furthermore, reducing intensity of a high-intensity image in the *eHSI* space will always produce a better enhancement result than in the *HSI* space.

8. **Conclusions.** *HSI* is a perceptual color model; many applications on color image enhancement, segmentation and recognition have been developed based on this color model. *HSI* model is cylindrical coordinate system; many color models of Cartesian coordinate systems, including *CIELAB* and *CIELUV* models, can certainly be transformed to their *HSI* models, respectively. The main purpose of this study is to improve the traditional *HSI* model for variant applications on color images, not to compare enhancement results.

The proposed *eHSI* color model has several advantages over the traditional *HSI* color model. First, the model has no out-of-gamut problem and the intensity component can be changed faithfully. As mentioned in the introduction section, Weeks et al. [23] suggested hue-preserving color image enhancement techniques that partition the whole (C-Y) color space into $N \times K$ subspaces, where N and K are the number of partitions in the luminance and saturation components, respectively. However, the decision of the subspace numbers N and K is crucial to the results. Duan and Qiu [6] stated that the more the regions were divided, the fewer cross-session artifacts there are, but more computational time is needed. Moreover, the calculation of lookup table is complicated. Here, the proposed *eHSI* model need not consider the subspace division and create lookup tables. Of course, we can also divide the *eHSI* color space into subspaces and enhance each subspace separately without the out-of-gamut problem and lookup table calculation.

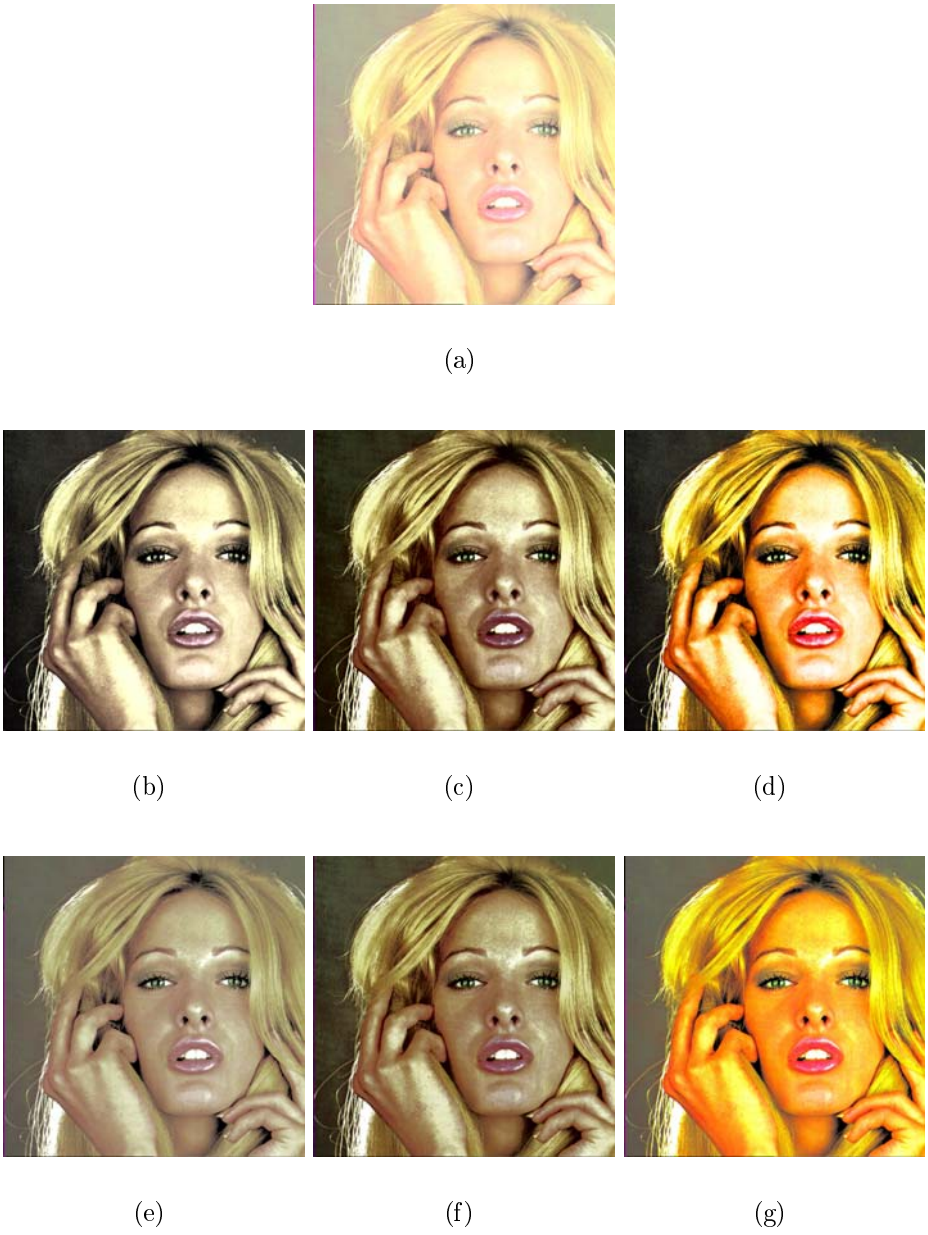

(a)

(b) (c) (d)

(e) (f) (g)

FIGURE 10. The enhanced results of Tiffany image: (a) the original image; (b) (c) (d) intensity histogram is equalized in *HSI*, *CIELAB* and *eHSI* spaces, respectively; (e) (f) (g) intensity histogram is centralized by *S-type* transformation in *HSI*, *CIELAB* and *eHSI* spaces, respectively

Second, the saturation component is automatically adjusted according to the attainable maximum saturation range. Hence, the saturation enhancement is simultaneously achieved with the intensity enhancement. Most color image enhancement procedures enhance intensity and saturation separately so that the correlation between intensity and saturation is destroyed and some abnormal patches are appeared. For some color image enhancement algorithms in the traditional *HSI* model, the achromatic region must be specially treated to avoid the over-enhancement problem. Contrarily, in the *eHSI* space, the saturation is automatically adjusted according to its attainable maximum saturation

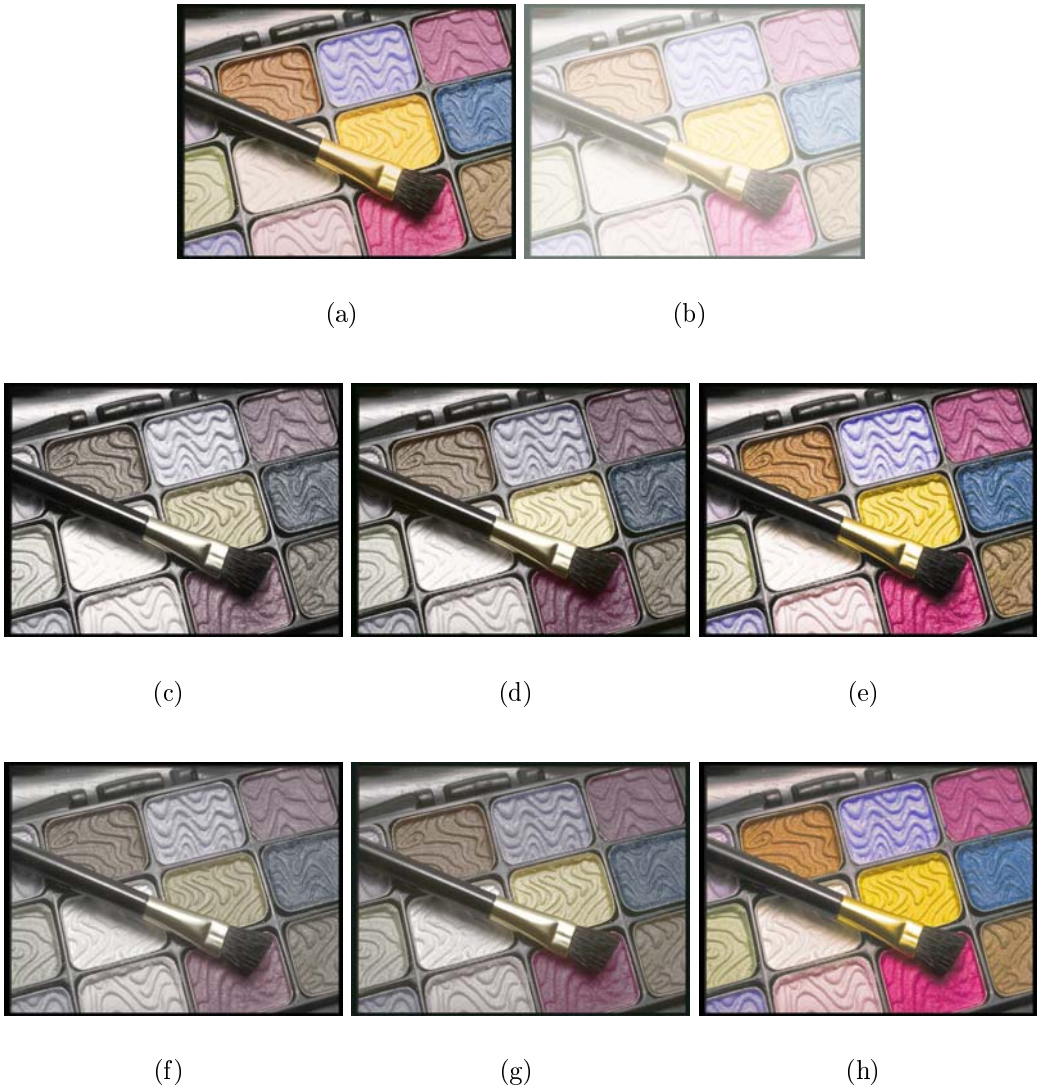

(a) (b)

(c) (d) (e)

(f) (g) (h)

FIGURE 11. The enhanced results of the brightened cosmetic image: (a) the original image; (b) the brightened image; (c) (d) (e) intensity histogram is equalized in *HSI*, *CIELAB* and *eHSI* spaces, respectively; (f) (g) (h) intensity histogram is centralized by *S-type* transformation in *HSI*, *CIELAB* and *eHSI* spaces, respectively

range. With the suggested *S-type* transformation method, the intensity is mildly adjusted toward the intensity central region, and the attainable maximum saturation range is mildly expanded; hence, over-enhancement of saturation in the achromatic region rarely occurs.

Third, in the traditional *HSI* space, the saturation is always reduced if the intensity is decreased and the saturation is always increased if the intensity is increased. Furthermore, the intensity increasing is disrupted if the pixel is out of gamut. However, these problems are totally solved in the proposed *eHSI* space.

Naik and Murthy [21] proposed an effective method for handling the out-of-gamut problem during color processing. The processing is completely done in the *RGB* space; thus, there is no need to back the *RGB* values to their bounds after the processing. Moreover, the saturation and hue values of pixels need not be processed, but the hue is

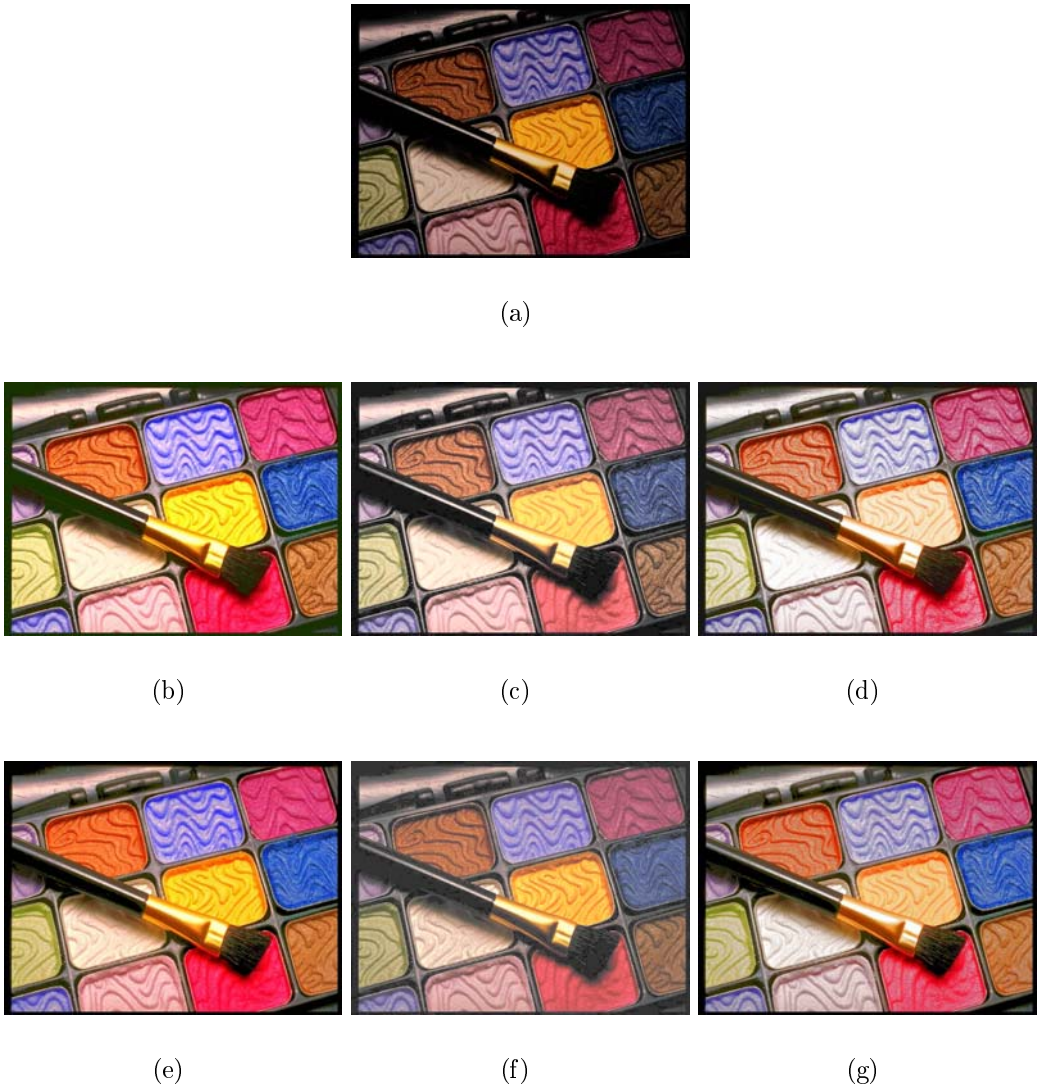

(a)

(b) (c) (d)

(e) (f) (g)

FIGURE 12. The enhanced results of the darkened cosmetic image: (a) the darkened image; (b) (c) (d) intensity histogram is equalized in *HSI*, *CIELAB* and *eHSI* spaces, respectively; (e) (f) (g) intensity histogram is centralized by *S-type* transformation in *HSI*, *CIELAB* and *eHSI* spaces, respectively

preserved. However, several enhancement algorithms developed in the *HSI* space cannot be used by this method. On the other hand, manipulating intensity and saturation in the *RGB* space requires far less intuition than that in the *HSI* space.

The computational burden of the proposed *eHSI* transformation is not much higher than that of the traditional *HSI* transformation because the extra load is just a few decision criteria. Though *HSI* and *eHSI* transformations have the similar computational complexity, they are still more complicated than *HSV* color model. *HSV* color model is more popular and simpler computation than *HSI* color model. We will analyze the *HSV* properties and evaluate whether it is more suitable for color image enhancement or not in the future.

REFERENCES

[1] R. C. Gonzalez and R. E. Woods, *Digital Image Processing*, 3rd Edition, Prentice Hall, Upper Saddle River, NJ, 2007.

[2] T. Tateyama, Z. Nakao, X. Han and Y.-W. Chen, Contrast enhancement of MR brain images by canonical correlations based kernel independent component analysis, *International Journal of Innovative Computing, Information and Control*, vol.5, no.7, pp.1857-1866, 2009.

[3] Md. F. Hossain and M. R. Alsharif, Minimum mean brightness error dynamic histogram equalization for brightness preserving image contrast enhancement, *International Journal of Innovative Computing, Information and Control*, vol.5, no.10(A), pp.3263-3274, 2009.

[4] J. Pan, C. Zhang and Q. Guo, Image enhancement based on the shearlet transform, *ICIC Express Letters*, vol.3, no.3(B), pp.621-626, 2009.

[5] Y. Zhang, C. Zhang, J. Chi and R. Zhang, An algorithm for enlarged image enhancement, *ICIC Express Letters*, vol.3, no.3(B), pp.669-674, 2009.

[6] J. Duan and G. Qiu, Novel histogram processing for colour image enhancement, *Proc. of the 3rd Int. Conf. on Image and Graphics*, Hong Kong, pp.55-58, 2004.

[7] G. J. Chamberlin, *The CIE International Colour System Explained*, 2nd Edition, The Tintometer Ltd., Salisbury, England, 1955.

[8] R. N. Strickland, C. Kim and W. F. McDonnell, Digital color image enhancement based on the saturation component, *Optical Engineering*, vol.26, pp.609-616, 1987.

[9] B. A. Thomas, R. N. Strickland and J. J. Rodriguez, Color image enhancement using spatially adaptive saturation feedback, *Proc. of Int. Conf. on Image Processing*, Santa Barbara, CA, USA, vol.3, pp.30-33, 1997.

[10] A. Toet, Multiscale color image enhancement, *Proc. of Int. Conf. on Image Processing and Its Application*, Maastricht, Netherlands, pp.583-585, 1992.

[11] I. Pitas and P. Kiniklis, Multichannel techniques in color image enhancement and modeling, *IEEE Trans. on Image Processing*, vol.5, no.1, pp.168-171, 1996.

[12] P. E. Trahanias and A. N. Venetsanopoulos, Color image enhancement through 3-D histogram equalization, *Proc. of the 11th IAPR Int. Conf. on Pattern Recognition*, The Hague, Netherlands, vol.3, pp.545-548, 1992.

[13] P. A. Mlsna and J. J. Rodriguez, A multivariate contrast enhancement technique for multispectral images, *IEEE Trans. on Geoscience and Remote Sensing*, vol.33, no.1, pp.212-216, 1995.

[14] P. A. Mlsna, Q. Zhang and J. J. Rodriguez, 3-D histogram modification of color images, *Proc. of Int. Conf. on Image Processing*, Lausanne, Switzerland, pp.1015-1018, 1996.

[15] Q. Zhang, P. A. Mlsna and J. J. Rodriguez, A recursive technique for 3-D histogram enhancement of color images, *Proc. of the IEEE Southwest Symp. on Image Analysis and Interpretation*, San Antonio, TX, USA, pp.218-223, 1996.

[16] I. M. Bockstein, Color equalization method and its application to color image processing, *J. Opt. Soc. Am. A*, vol.3, pp.735-737, 1986.

[17] A. R. Weeks, G. E. Hague and H. R. Myler, Histogram equalization of 24-bit color images in the color difference (C-Y) color space, *Journal of Electronic Imaging*, vol.4, pp.15-22, 1995.

[18] C. C. Yang and J. J. Rodriguez, Efficient luminance and saturation processing techniques for bypassing color coordinate transformations, *Proc. of IEEE Int. Conf. on Systems, Man and Cybernetics*, Vancouver, BC, Canada, pp.667-672, 1995.

[19] C. C. Yang and J. J. Rodriguez, Saturation clipping in the LHS and YIQ color spaces, *Proc. of Conf. on Color Imaging: Device-Independent Color, Color Hard Copy, and Graphic Arts*, San Jose, CA, USA, pp.297-307, 1996.

[20] J. J. Rodriguez and C. C. Yang, High-resolution histogram modification of color images, *Graphical Models and Image Processing*, vol.57, pp.432-440, 1995.

[21] S. K. Naik and C. A. Murthy, Hue-preserving color image enhancement without gamut problem, *IEEE Trans. on Image Processing*, vol.2, no.12, pp.1591-1598, 2003.

[22] M.-S. Shyu and J.-J. Leou, A genetic algorithm approach to color image enhancement, *Pattern Recognition*, vol.31, pp.871-880, 1998.

[23] A. R. Weeks, L. J. Sartor and H. R. Myler, Histogram specification of 24-bit color images in the color difference (C-Y) color space, *Journal of Electronic Imaging*, vol.8, pp.290-300, 1999.